

LA-UR-21-23361

Approved for public release; distribution is unlimited.

Title: PBX9012 Tracker Gauge Data

Author(s): Menikoff, Ralph

Intended for: Technical note for colleagues and coworkers

Issued: 2021-04-08

Disclaimer:

Los Alamos National Laboratory, an affirmative action/equal opportunity employer, is operated by Triad National Security, LLC for the National Nuclear Security Administration of U.S. Department of Energy under contract 89233218CNA000001. By approving this article, the publisher recognizes that the U.S. Government retains nonexclusive, royalty-free license to publish or reproduce the published form of this contribution, or to allow others to do so, for U.S. Government purposes. Los Alamos National Laboratory requests that the publisher identify this article as work performed under the auspices of the U.S. Department of Energy. Los Alamos National Laboratory strongly supports academic freedom and a researcher's right to publish; as an institution, however, the Laboratory does not endorse the viewpoint of a publication or guarantee its technical correctness.

PBX9012 TRACKER GAUGE DATA

RALPH MENIKOFF

April 7, 2021

1 Introduction

Five shock-to-detonation transition (SDT) gas gun experiments for PBX 9012 were performed by [Burns and Chiquete \[2020\]](#). The data from the experiments is available on the small-scale database. Here we focus on the tracker gauge data for the lead shock trajectory, $x(t)$.

In order to determine the shock speed $U_s(t)$ and the detonation transition point, a least squared fit to the shock trajectory is used based on a pair of ODEs with a fitting form for the shock acceleration developed by [Hill and Gustavsen \[2002\]](#).

$$\frac{d}{dt} \begin{pmatrix} x \\ U_s \end{pmatrix} = \begin{pmatrix} U_s \\ a_m \frac{D-U_s}{D-U_m} \exp\left(\frac{U_s-U_m}{D-U_m}\right) \end{pmatrix}, \quad (1)$$

where U_s is the shock speed, and the fitting form parameters are the final shock speed D , the shock speed at maximum acceleration U_m and the maximum acceleration a_m . There are also two parameters for the initial conditions of the ODEs; $x_0 = x(t_0)$ and $u_s = U_s(t_0)$. Two common criterion for the transition point are (i) the point of maximum acceleration (*i.e.*, $U_s = U_m$), and (ii) the point at which the shock speed U_s is 95 percent of the final speed D (*i.e.*, $U_s = 0.95 D$).

The trajectory data are from 3 tracker gauges (left, right and center) and the time of arrival of the lead shock for up to 9 velocity gauges and a stirrup gauge at the front surface of the HE which is used to set the time origin; see [[Burns and Chiquete, 2020](#), fig 1]. The different gauges have overlapping domains and provide some redundancy for lost data points due to noisy signals.

A previous note on the shock trajectory for shot 1s-1674 [[Menikoff, 2021c](#)] showed that the detonation transition point varied when different combinations of tracker gauges were used to fit the shock trajectory. This is due to time offsets for data points with corresponding positions on the different gauges. In particular, there is a significant change in the transition point when the center gauge data points are left out, even though all the center gauge data points are significantly after the transition. The time offsets are due partly to tilt [see [Menikoff, 2021b](#), and references therein] and partly to the variable thickness of the glue joints between the gauge package and the HE [see [Menikoff, 2021a](#)].

In the next section, fits to the trajectory data for all five experiments are examined and observation that can affect the accuracy of the shock speed and detonation transition point are discussed.

2 Fits to trajectory data

The trajectory data and fits for each experiment are shown in fig. 1, and the fitting parameters listed in table 1. Along with the fit to the data, the plots in fig. 1 show the residual of the fit; $\text{residual}(t) = x(t) - x_{fit}(t)$. The residual for the middle plots is color coded by tracker gauge. It can be seen that there are significant offsets in the residuals between the different gauges. Moreover, the offsets for each gauge are not constant and not random. Combining data from gauges with different offsets is a significant source of uncertainty in the shock speed derived from the ODE fit to the shock trajectory.

Both the table and figure show the shots in decreasing order of initial shock strength based on the speed of the gas gun projectile [Burns and Chiquete, 2020, table IV] driving the SDT. The ordering is consistent with the values of the detonation transition point from the trajectory fits. However, it is not consistent with the parameter $U_s(0)$ for the initial shock speed (which should be monotonically increasing with shock strength) shown in the table.

We note that the first tracker data point is downstream of the front surface of the HE. Thus, $U_s(0)$ represents an extrapolation of the shock trajectory data based on the assumed fitting form for the shock acceleration in a regime of shock speeds much lower than the 3 fitting parameters D , U_m and a_m are most sensitive to.

As a check on the fits, table 1 shows for shot 2s-1101 both the parameters listed in [Burns and Chiquete, 2020, table VI] and the parameters for the fit we obtained. The two parameter

Table 1: ODE parameters for fits to PBX 9012 shots. RMS is the root mean squared of the residual. t_* and x_* are transition point from maximum acceleration criteria. Gauges are abbreviated as s and g , for stirrup and velocity gauges, and l , r , c for left, right and center tracker gauges, respectively.

shot	gauges	x_0 mm	$U_s(0)$ km/s	D km/s	U_m km/s	a_m mm/ μ s ²	RMS μ m	$\frac{D-D_{cj}}{D_{cj}}$ percent	t_* μ s	x_* mm
2s-1101 [#]	sglrc	-0.010	3.32	8.97	7.55	10.93	49	4.3	0.835	4.028
2s-1101*	sglrc	-0.014	3.354	8.970	7.602	11.48	45	4.3	0.845	4.074
2s-1101 ^{*a}	$t < 1.2$	-0.031	3.468	8.790	7.601	13.45	52	2.2	0.834	3.988
1s-1673*	sglrc	-0.121	3.550	8.987	8.438	317.3	75	4.5	1.457	5.977
1s-1684*	sgc [†]	0.035	3.351	8.593	8.207	4000 [‡]	21	-0.8	2.314	8.932
1s-1674*	sglrc	0.117	2.744	9.785	8.805	26.56	147	13.8	2.996	11.934
1s-1674 ^{*b}	sglr	0.038	3.011	8.328	7.703	54.92	87	-3.2	2.827	10.655
1s-1675*	sglrc	0.052	2.893	5.710 [‡]	5.333	7.49	92	-33.6	5.239	17.619

[#] fit parameters from Burns and Chiquete [2020, table VI]

* middle plot in fig. 1

^{*a} comparison in fig. 4

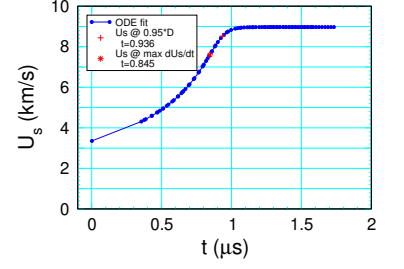
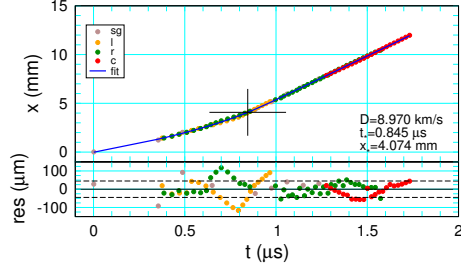
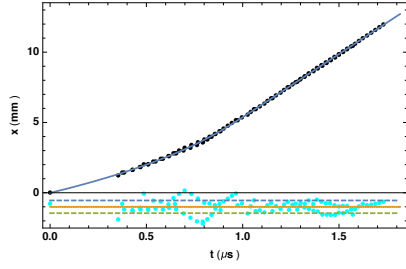
[†] no data for left and right tracker gauges

[‡] fit insensitive to large a_m due to coarse data before transition

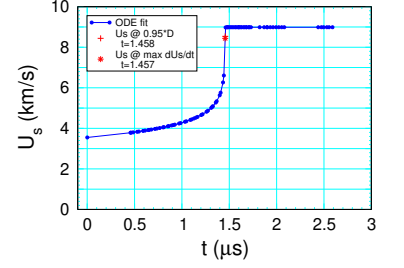
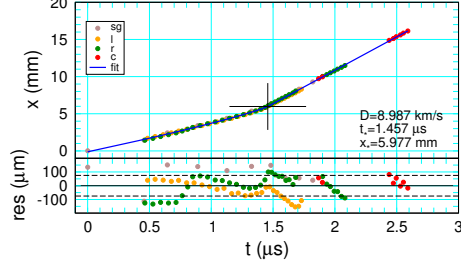
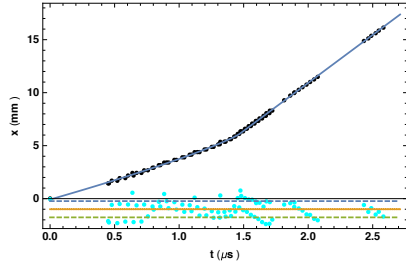
^{*b} comparison in fig. 5

[‡] low velocity detonation, see [Stewart and Yao, 1998]

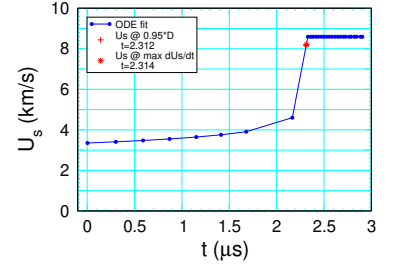
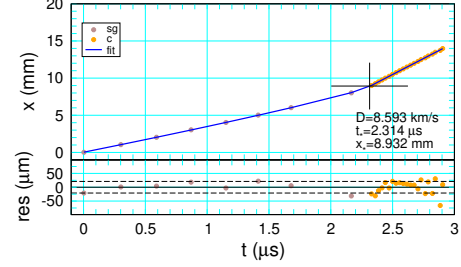
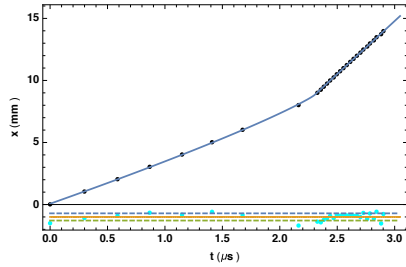
shot
2s-1101



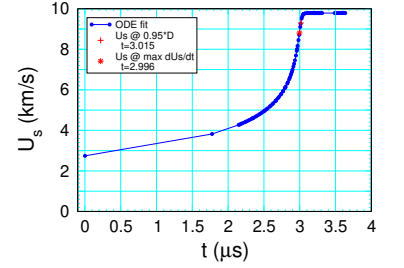
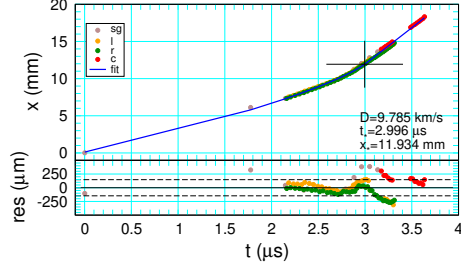
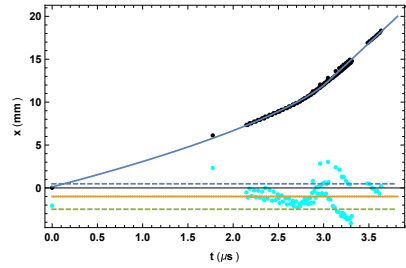
shot
1s-1673



shot
1s-1684



shot
1s-1674



shot
1s-1675

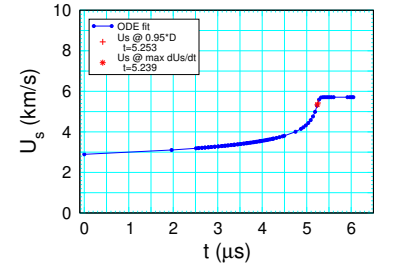
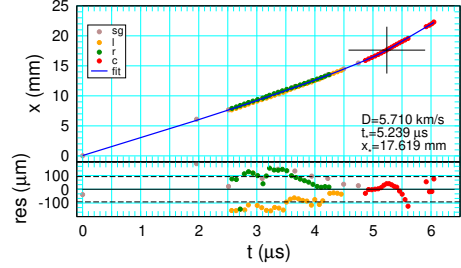
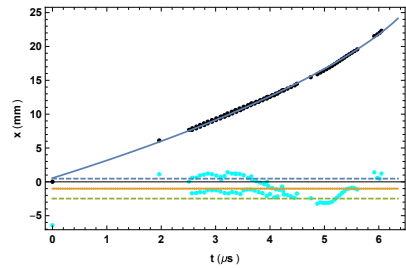


Figure 1: Shock trajectory from ODE fit to tracker gauges for the 5 PBX 9012 shots. Left plots from Burns & Chiquete on small-scale database. On middle plots, cross hair indicate point of maximum shock acceleration. Bottom of trajectory plots are the residual of fit, $x(t) - x_{fit}(t)$; 10 times scale for left plots, and color coded by tracker gauge for middle plots (sg, l, r, c for stirrup plus velocity gauges, left, right and center trackers, respectively.) Dashed lines indicate \pm root mean square of the residual. Right plots are the lead shock speed time history corresponding to the middle plots. Red symbols are transition points for two transition criterion.

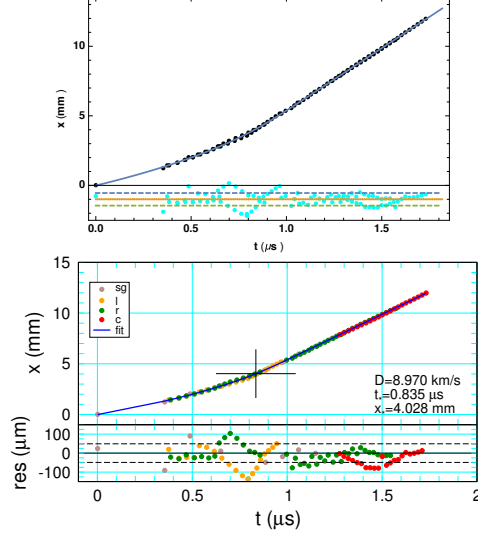


Figure 2: Comparison of shock trajectories for shot 2s-1101 with fitting parameters listed in [Burns and Chiquete, 2020, table VI]. The top plot is from the small-scale database and the bottom plot uses trajectory data from the small-scale database.

sets are slightly different, even though both fits used the data from all the tracker gauges. A comparison of the two trajectory fits is shown in fig. 2. Close inspection of the residuals indicates that 3 trajectory points at late time were left out of the tracker data file. Other than as a check, the small differences in the fitting parameters are not significant.

The difference in shock velocities between the ODE fit and a tracker gauge are related to the slope of the residual, $U_s(t) = U_{fit}(t) - \frac{d}{dt}\text{residual}$. As an illustrative example, the slope of the residual for the left (orange) tracker of shot 2s-1101 over the time interval $0.8 < t < 1.0 \mu\text{s}$ is approximately $1 \text{ mm}/\mu\text{s}$ or 12 percent of D . In this time interval, the slope of the residual for the right (green) tracker has a similar magnitude but with the opposite sign.

The fact that the residuals of a gauge has a well define slope over some time intervals implies that the uncertainties in neighboring data points are correlated. The PBX 9012 shots are unusual in that the thickness of the glue joints between the gauge package and the HE are larger than normal. The correlations may be due to long wavelength variations in the glue joint thickness.

We note that the gas gun experiments are nominally one-dimensional. In 1-D, the underdriven or CJ detonation speed is determined by the products EOS. For PBX 9012, the CJ detonation speed inferred from rate stick experiments is $D_{cj} = 8.60 \text{ km/s}$. Simulations of the SDT experiments in 1-D show that the transition to detonation is very abrupt. Moreover, within 2 mm of the transition, the speed of the lead shock is nearly D_{cj} . Both effects are due to the large burn rate at shock speeds in the detonation wave regime; *i.e.*, U_s near D_{cj} . The large burn rate is needed for a narrow reaction-zone width (less than 0.1 mm) required to match the small curvature effect inferred from PBX 9012 rate stick experiments.

The transition to a detonation is abrupt when the slope of the shock trajectory in the neighborhood of the transition is large. As a consequence, the transition point is insensitive to the

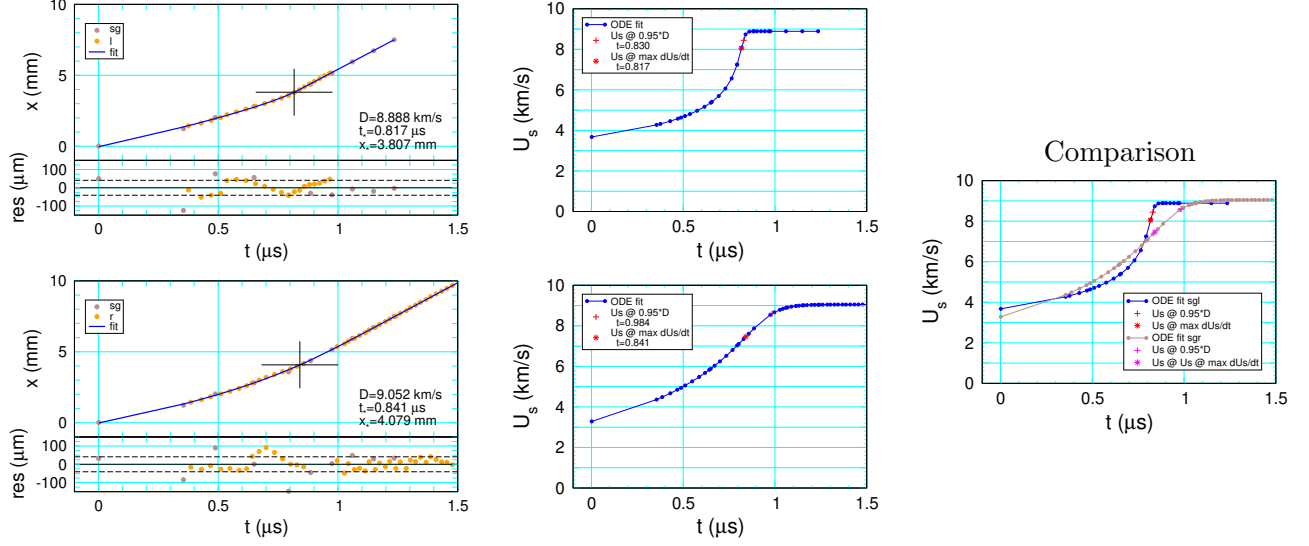


Figure 3: Comparison of fits for 2s-1101; left tracker (top plots), and right tracker (bottom plots).

transition criterion. For the ODE fit to the shock trajectory, the abruptness of the transition depends on the parameter for the maximum acceleration. As seen in the tracker fits shown in fig. 1, the transition is reasonably abrupt when $a_m > 20 \text{ mm}/\mu\text{s}^2$. This covers 4 of the 5 shots, the exception being 2s-1101.

The variation or scatter in the trajectory data can reduce the value a_m . In general, the maximum acceleration for an ideal 1-D SDT is expected to be larger than the value for a nominally 1-D experiment. There is also a sensitivity of the fits to small correlated variations in the data which shows up most strongly in time history of the shock velocity. As an illustrative example, fig. 3 shows a comparison of fits for shot 2s-1101 using the velocity gauges and the left vs right tracker gauges. The RMS residual of both fits are about $41 \mu\text{m}$, but a_m is 38 and $9 \text{ mm}/\mu\text{s}^2$ for the left and right tracker fits, respectively. The figure shows a significant difference in $U_s(t)$, which affects the transition point and gives an 11 percent difference in the initial shock speed.

Unlike simulations, the fits to the trajectory data have a final shock speed (parameter D) that can differ significantly from D_{cj} . From table 1, shot 1s-1764 is an extreme case with D 14 percent larger than D_{cj} , even though the data extends after the transition by over 5 mm and $0.5 \mu\text{s}$. For the more typical cases, D differs from D_{cj} by up to 4.5 per cent.

We note that misalignment can lead to a scaling of the gauge positions [see Menikoff, 2021b, and references therein] which would affect the shock speed. Though the tilt angle was not measured for the PBX 9012 shots, estimates of error in the shock speed is only up to 2 percent. Since this is smaller than the differences shown in table 1, we consider other causes for the discrepancy.

Figure 4 shows a comparison of the fits for shot 2s-1101 when the data is cutoff at $t = 1.2 \mu\text{s}$. The cutoff is $0.36 \mu\text{s}$ after the detonation transition and largely serves to exclude the center tracker. It reduce D by 2 percent and gives a slightly earlier detonation transition. The largest

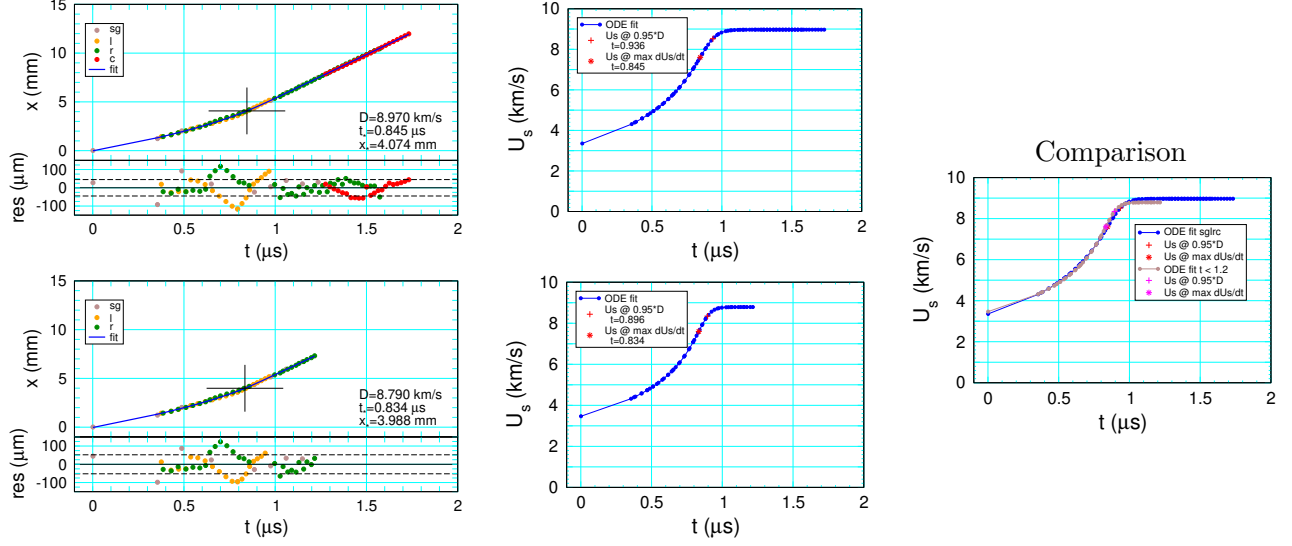


Figure 4: Comparison of fits for 2s-1101; all tracker data (top plots), and data limited to $t < 1.2 \mu$ (bottom plots).

effect is a 3.4 percent increase in initial shock speed. This case shows that data long after the transition can affect the shock speed from the fit by a few percent.

The trajectory plot for shot 1s-1674 in fig. 1 shows that the center tracker has a significant offset. Figure 5 shows a comparison of tracker fits with and without the center tracker data. Without the center tracker, D decreases by 10 percent, the initial shock speed increases by 9 percent, and the RMS residual decreases by 40 percent. Moreover, the transition is more abrupt (since a_m is twice as large) leading to a significant decrease in the detonation transition point (10 and 5.6 percent in run distance and time to detonation, respectively), and a significant shift in $U_s(t)$. Thus, the offset in a tracker gauge after the detonation transition can have a significant adverse effect on the shock speed inferred from the ODE fit to the shock trajectory data.

Shot 1s-1675 has the lowest initial shock pressure. Its shock trajectory, shown in fig. 1, is anomalous. The final shock speed is 34 percent below D_{cj} . However, the shock speed is constant for the last 0.8μ s and 5 mm of run. This suggests that the shock has transitioned to a low velocity detonation after 17.6 mm of run. Since the planar CJ detonation is unique, a low velocity detonation requires a curved detonation front; see [Stewart and Yao, 1998]. Possibly, variations in the glue joint thickness with the gauge package triggered the non-planarity of the lead shock.

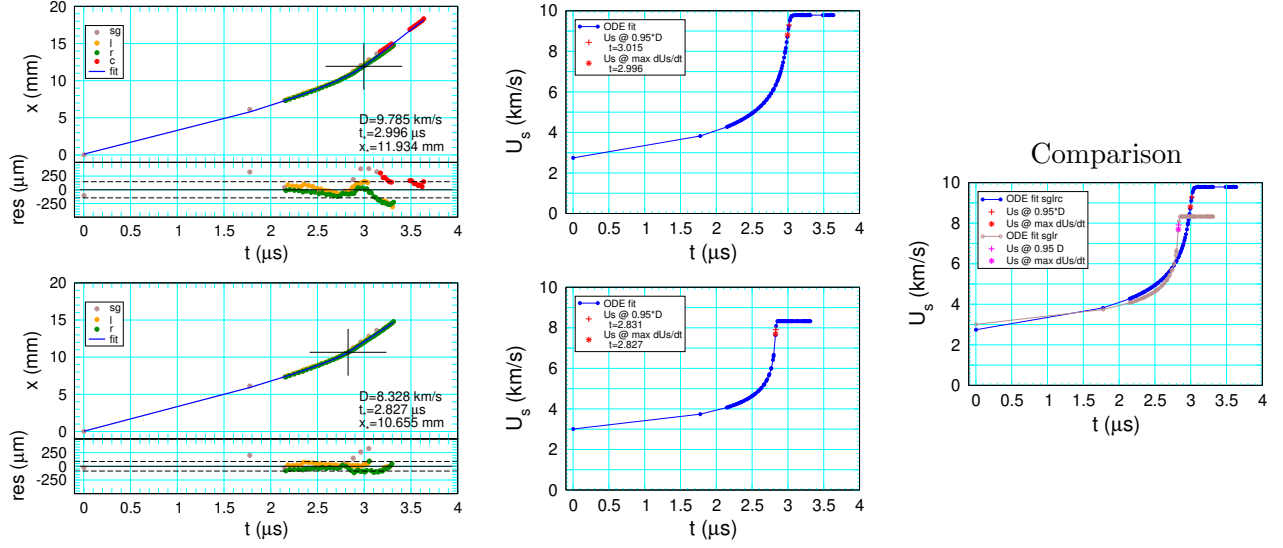


Figure 5: Comparison of fits for 1s-1674; all tracker data (top plots), and without center tracker (bottom plots).

3 Final remarks

One of the intents of the ODE fits is to make the determination of the detonation transition point less subjective by using a well defined algorithm. This maybe true if the tracker data uncertainty is small and random. However, the PBX 9012 tracker data illustrates that there are several gotchas, especially with variable offsets among the different tracker gauges.

Several things to watch out for:

1. The parameter a_m should be sufficiently large for an abrupt transition to detonation as viewed in a plot of $U_s(t)$. Otherwise, the transition point can be sensitive to the transition criteria.
2. The parameter for the final shock speed D should be within a few percent of the CJ detonation speed. Otherwise, the trajectory fit can be sensitive to data long after the transition point.
3. The initial shock speed $U_s(0)$ may have a large uncertainty due to extrapolating the trajectory fit to the front surface of the HE. This would affect the determination of the initial shock pressure based on the shock jump condition $P = \rho_0 u_p u_s$ with u_p inferred from the stirrup gauge.

References

- M. J. Burns and C. Chiquete. Shock initiation of the HMX-based explosive PBX 9012: Experiments, uncertainty analysis, and unreacted equation-of-state. *J. Appl. Phys.*, 127:215107, 2020. URL <https://doi.org/10.1063/1.5144686>.
- L. G. Hill and R. L. Gustavsen. On the characterization and mechanisms of shock initiation in heterogeneous explosives. In *Proceeding of the Twelfth International Symposium on Detonation*, pages 975–987, 2002.
- R. Menikoff. xRage simulations of magnetic velocity gauges used in gas gun shock initiation experiments. Technical Report LA-UR-21-21769, Los Alamos National Lab., 2021a.
- R. Menikoff. Magnetic velocity gauges: Effects of misalignment. Technical Report LA-UR-21-22095, Los Alamos National Lab., 2021b.
- R. Menikoff. Tracker fits for shot 1s1674. Technical Report LA-UR-21-22603, Los Alamos National Lab., 2021c.
- D. S. Stewart and J. Yao. The normal detonation shock velocity-curvature relation for materials with non-ideal equations of state and multiple turning points. *Combustion and Flame*, 113: 224–235, 1998. URL [https://doi.org/10.1016/S0010-2180\(97\)00170-3](https://doi.org/10.1016/S0010-2180(97)00170-3).